JBC ARTICLE

⌘ Author's Choice

A transient amphipathic helix in the prodomain of PCSK9 facilitates binding to low-density lipoprotein particles

Received for publication, July 18, 2019, and in revised form, January 13, 2020 Published, Papers in Press, January 16, 2020, DOI 10.1074/jbc.RA119.010221

Samantha K. Sarkar[‡], Alexander C. Y. Foo[§], Angela Matyas[‡], Ikhuosho Asikhia[‡], Tanja Kosenko[‡], Natalie K. Goto[§], Ariela Vergara-Jaque[¶‖1], and Thomas A. Lagace[‡2]

From the [‡]Department of Biochemistry, Microbiology and Immunology, University of Ottawa Heart Institute, Ottawa, Ontario K1Y 4W7, Canada, the [§]Department of Chemistry and Biomolecular Sciences, Faculty of Science, University of Ottawa, Ottawa, Ontario K1N 6N5, Canada, the [¶]Center for Bioinformatics and Molecular Simulation, Universidad de Talca, 3460000 Talca, Chile, and the [‖]Millennium Nucleus of Ion Channels-associated Diseases (MiNICAD), 3460000 Talca, Chile

Edited by Phyllis I. Hanson

Proprotein convertase subtilisin/kexin type-9 (PCSK9) is a ligand of low-density lipoprotein (LDL) receptor (LDLR) that promotes LDLR degradation in late endosomes/lysosomes. In human plasma, 30–40% of PCSK9 is bound to LDL particles; however, the physiological significance of this interaction remains unknown. LDL binding *in vitro* requires a disordered N-terminal region in PCSK9's prodomain. Here, we report that peptides corresponding to a predicted amphipathic α-helix in the prodomain N terminus adopt helical structure in a membrane-mimetic environment. This effect was greatly enhanced by an R46L substitution representing an atheroprotective *PCSK9* loss-of-function mutation. A helix-disrupting proline substitution within the putative α-helical motif in full-length PCSK9 lowered LDL binding affinity >5-fold. Modeling studies suggested that the transient α-helix aligns multiple polar residues to interact with positively charged residues in the C-terminal domain. Gain-of-function *PCSK9* mutations associated with familial hypercholesterolemia (FH) and clustered at the predicted interdomain interface (R469W, R496W, and F515L) inhibited LDL binding, which was completely abolished in the case of the R496W variant. These findings shed light on allosteric conformational changes in PCSK9 required for high-affinity binding to LDL particles. Moreover, the initial identification of FH-associated mutations that diminish PCSK9's ability to bind LDL reported here supports the notion that PCSK9-LDL association in the circulation inhibits PCSK9 activity.

Circulating liver-derived proprotein convertase subtilisin/kexin type-9 (PCSK9)[3] is a leading drug target in cardiovascular medicine due to its ability to bind and mediate degradation of hepatic LDL receptor (LDLR), the primary conduit for the clearance of plasma LDL-cholesterol (LDL-C) (1–3). Gain-of-function (GOF) mutations in *PCSK9* result in familial hypercholesterolemia (FH), whereas loss-of-function (LOF) mutations are associated with life-long reductions in plasma LDL-C and significant protection from cardiovascular heart disease (4–6). Therapeutic monoclonal antibodies that target PCSK9 and prevent its binding to LDLR lower LDL-C by up to 70% in hypercholesterolemic patients, clearly establishing circulating PCSK9 as a central regulator of hepatic LDLR expression and plasma LDL-C levels (7, 8).

PCSK9 is a member of the mammalian proprotein convertase family of serine proteases related to bacterial subtilisin and yeast kexin (9). Human PCSK9 is a 692-residue secreted protein consisting of a 30-residue signal sequence followed by a prodomain, a subtilisin-like catalytic domain, and a C-terminal cysteine-histidine–rich (CHR) domain (Fig. 1*A*). Autocatalytic processing in the endoplasmic reticulum releases the prodomain, which remains noncovalently bound and blocks substrate access to the active site, rendering mature PCSK9 catalytically inert (10, 11). Like LDL, plasma PCSK9 clearance is predominantly via LDLR-mediated endocytosis in liver (12, 13). The apolipoprotein B100 (apoB100) moiety of LDL binds to the ligand-binding domain of LDLR and undergoes acid-dependent release in early endosomes, allowing LDLR to recycle to the cell surface (14, 15). In contrast, PCSK9 binds to the first epidermal growth factor (EGF)-like repeat (EGF-A) in the EGF precursor homology domain of LDLR and with higher affinity at acidic pH (16); thus, PCSK9 fails to release in early endosomes and directs LDLR for degradation in late endosomes/lysosomes (3, 10, 17).

Approximately 30–40% of PCSK9 in normolipidemic human plasma is bound to LDL particles (13, 18). Co-immunoprecipitation experiments have confirmed a protein-protein interaction between PCSK9 and apoB100, the main protein

This work was supported in part by Heart and Stroke Foundation of Canada Grant G-15-0009352, Canadian Institutes of Health Research (CIHR) Grant 391063, and the Pfizer ASPIRE Program (to T. A. L.). The authors declare that they have no conflicts of interest with the contents of this article.

This article contains Table S1 and Figs. S1 and S2.

[1] Supported by FONDECYT Research Initiation Grant 11170223. The Millennium Nucleus of Ion Channels-Associated Diseases (MiNICAD) is a Millennium Nucleus supported by the Iniciativa Científica Milenio of the Ministry of Economy, Development, and Tourism (Chile).

[2] To whom correspondence should be addressed: Dept. of Biochemistry, Microbiology, and Immunology, University of Ottawa Heart Institute, 40 Ruskin St., Rm. H-4213, Ottawa, Ontario K1N 6N5, Canada. Tel.: 613-696-7356; Fax: 613-696-7130; E-mail: tlagace@ottawaheart.ca.

[3] The abbreviations used are: PCSK9, proprotein convertase subtilisin/kexin type 9; LDL, low-density lipoprotein; LDLR, LDL receptor; LDL-C, LDL-cholesterol; apo, apolipoprotein; FH, familial hypercholesterolemia; GOF, gain-of-function; LOF, loss-of-function; IDR, intrinsically disordered region; AH, amphipathic helix; EGF, epidermal growth factor; CHR domain, cysteine-histidine–rich domain; CM1, CHR domain module 1; aa, amino acids; DPC, *n*-dodecylphosphocholine; PDB, Protein Data Bank; AAD, acidic activation domain; NCLPDS, newborn calf lipoprotein-deficient serum; LDLR-ECD, LDLR extracellular domain.

component of human LDL (18, 19), and PCSK9 has also been shown to bind apoB within the secretory pathway in hepatocytes (20). PCSK9-LDL binding *in vitro* is saturable and specific with a K_D of ~125–350 nM (18, 21), which is within a range of affinities reported for the PCSK9-LDLR interaction (11, 22). Several studies have shown that LDL lowers PCSK9's ability to bind and mediate degradation of LDLRs in cultured cells (18, 22, 23). Conversely, there is evidence that LDL association promotes PCSK9-mediated LDLR degradation by inducing a more potent oligomeric form (13, 24) or by shielding PCSK9 from inactivating furin-mediated proteolysis (25). In sum, both the molecular mechanism of PCSK9-LDL binding and the physiological significance remain undefined.

We have previously mapped critical LDL-binding determinants *in vitro* to an intrinsically disordered region (IDR) in the N terminus of the PCSK9 prodomain (18). This region, unresolved in all available X-ray crystal structures of PCSK9 (11, 26), has also been identified as a negative allosteric effector of LDLR binding affinity (27, 28). A recent study demonstrated the existence of structural flexibility in the prodomain IDR whereby a mAb preferentially bound to a transient α-helix (29). Herein, we provide direct evidence demonstrating a functional role of such transient helical conformation in PCSK9-LDL association. Furthermore, computational modeling indicated an intramolecular interaction between the CHR domain and helical conformation of the prodomain IDR. This prompted an assessment of natural *PCSK9* mutations at or near this predicted interdomain interface. Our analysis revealed several FH-associated mutations in the CHR domain that greatly diminished (R469W and F515L) or abolished (R496W) the ability of PCSK9 to bind LDL *in vitro*. These data provide molecular insight into disease-causing mutations in the pathogenesis of FH and suggest that LDL association exerts an overall inhibitory effect on circulating PCSK9 activity.

Results

Identification of a putative amphipathic helix in N terminus of PCSK9

Fig. 1*B* shows the crystal structure of PCSK9 in complex with the EGF-A domain of LDLR (27) with emphasis on an IDR in the N terminus of the prodomain (aa 31–60 following the signal peptide cleavage site). We have previously mapped important LDL binding determinants to the N-terminal 21 amino acids in the IDR (18). Two sequences of interest are a highly acidic tract (aa 32–40; EDEDGDYEE) and an adjacent hydrophobic segment (aa 41–45; LVLAL) (Fig. 1*B*), both of which are evolutionarily well-conserved in mammals as well as other vertebrates (30) (Fig. S1). To test potential roles in LDL binding, plasmids encoding human PCSK9 with a deletion of residues 33–40 (leaving Gln-31 and Glu-32 intact for signal peptide cleavage) or replacement of the hydrophobic stretch and a neighboring Arg-46 residue with a glycine-serine linker were constructed and transfected into HEK293 cells. Secreted WT and mutant PCSK9 proteins present in the conditioned medium were then incubated with isolated human LDL particles followed by Optiprep density gradient ultracentrifugation to separate LDL-bound and unbound PCSK9. Deletion of the acidic tract (Δ33–40) nearly abolished PCSK9-LDL binding, whereas replacement of the hydrophobic residues with the Gly/Ser 41–46 linker reduced binding by >60% (Fig. 2, *A* and *B*), suggestive of a functional overlap between these sequences. As recently reported (29), secondary structure predictions using PSIPRED (31) showed an α-helical structure in this region with highest confidence for residues 38–45 (YEELVLAL) overlapping the acidic and hydrophobic segments (Fig. 2*C*). Helical wheel modeling revealed characteristics of an amphipathic α-helix (AH) for these residues, with a relatively polar face and an opposing face consisting of aromatic (Tyr-38) and nonpolar amino acids (Leu-41, Val-42, and Leu-45), giving the helix a directional hydrophobic moment (Fig. 2*D*) (32).

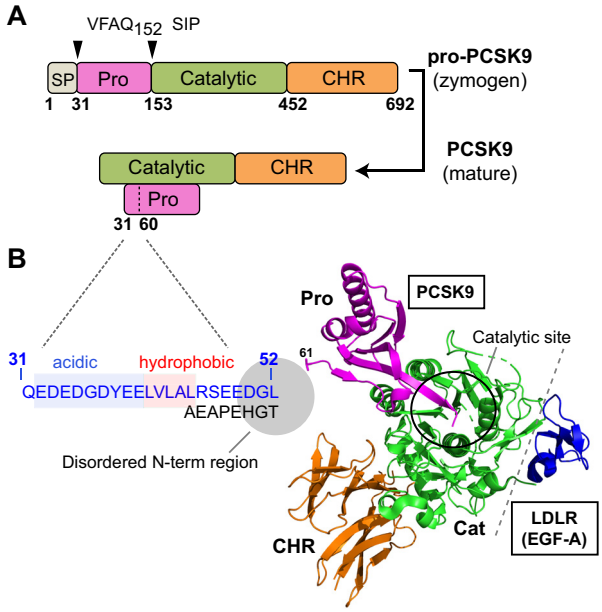

Figure 1. PCSK9 structure with emphasis on disordered N-terminal region of the prodomain. *A*, following removal of a signal peptide (*SP*; aa 1–30; *gray*), human pro-PCSK9 undergoes autocatalytic cleavage after Gln-152, resulting in mature PCSK9 consisting of a prodomain (aa 31–152; *magenta*), catalytic domain (aa 153–451; *green*), and C-terminal CHR domain (aa 452–692; *orange*). *B*, crystal structure of PCSK9 in complex with the EGF-A domain of LDLR (27) (PBD code 3BPS). The C-terminal end of the cleaved prodomain blocks the catalytic site (*black circle*), which is >20 Å from the binding interface with EGF-A (*gray dashed line*). An IDR in the N terminus of the prodomain (aa 31–60) (*shaded circle*) is structurally disordered and unobserved in all PDB-deposited crystal structures of PCSK9. *Highlighted* in *blue* is the amino acid sequence of an N-terminal region (aa 31–52) required for binding to LDL particles (18). Sequences of interest within this region are a highly acidic tract (*shaded blue*) and adjacent hydrophobic region (*shaded red*).

Amphipathic α-helix formation in a hydrophobic membrane-mimetic environment

Because the putative N-terminal helix is predicted to have amphipathic characteristics, a random coil-to-helix conformation change may be triggered in an amphipathic environment of a membrane surface, such as that present on lipoproteins. Therefore, we performed assessments of the secondary structure that this motif forms in aqueous *versus* membrane-mimetic conditions. Synthesized peptides corresponding to residues 37–47 (DYEELVLALRS) were dissolved in phosphate buffer or in buffer containing *n*-dodecylphosphocholine (DPC) micelles, a widely used membrane mimetic that can induce

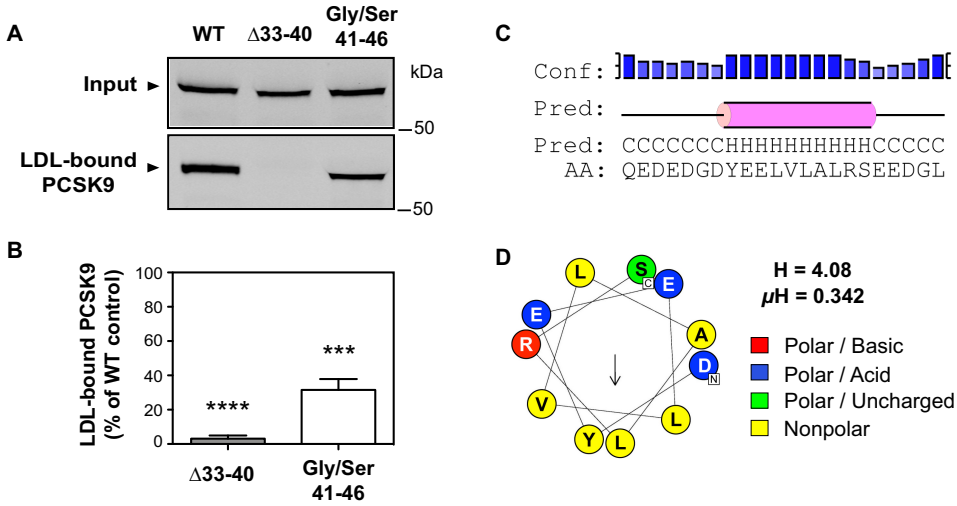

Figure 2. The PCSK9 N-terminal region is predicted to harbor an amphipathic α-helix. *A*, analysis of *in vitro* PCSK9-LDL binding reactions. Conditioned medium containing WT PCSK9 or variants lacking N-terminal acidic (Δ33–40) or hydrophobic (Gly/Ser 41–46) segments were incubated with LDL prior to density gradient ultracentrifugation to isolate an LDL fraction and visualization of bound PCSK9 by Western blotting. *B*, densitometric analyses of Western blotting in *A*. *Error bars*, S.E. ($n = 5$). Significant change in LDL binding compared with WT PCSK9 control (set to 100%) was determined by one-sample *t* test: ***, $p < 0.001$; ****, $p < 0.0001$. *C*, secondary structure prediction of PCSK9 aa 31–52 by PSIPRED. The prediction (*Pred*) shows helices (*H*) as *pink rods* and random coil (*C*) as a *black line*. The confidence level (*Conf*) is shown on the *top*. *Higher bars* with *darker shades of blue* represent higher prediction confidence. *D*, helical wheel representation of amphipathic α-helix (residues 37–47) generated from HeliQuest. The *arrow* indicates the magnitude and direction of the hydrophobic moment (32). The hydrophobicity (*H*) and hydrophobic moment (*μH*) from HeliQuest are also shown.

α-helical conformation in peptides with inherent amphipathic properties (33). CD spectra revealed that the motif remained in a random coil conformation in aqueous buffer but in the presence of DPC micelles adopted a distinctly helical conformation (Fig. 3*A*). Proline is a potential helix breaker due to a combination of steric constraints and the inability of the backbone imino group to participate in hydrogen bond formation. Accordingly, an A44P substitution in a prodomain-derivative peptide prevented a shift to helical conformation in the presence of DPC micelles (Fig. 3*B*).

Proline substitutions in the putative N-terminal helix greatly diminish PCSK9-LDL binding

To test the influence of peptide backbone conformation on LDL binding, we introduced proline residues at two separate positions in the putative helix (L41P and A44P) in full-length recombinant PCSK9 (Fig. 4*A*). In each case, proline substitution inhibited the ability of secreted PCSK9 to bind to LDL by >90% (Fig. 4*B*), supporting an important structural role of helical conformation in the prodomain N terminus. We have previously characterized that uptake of PCSK9 into cells is largely dependent on its cell surface interaction with LDLR (2). Accordingly, the addition of secreted WT PCSK9 to the culture medium of HEK293 cells overexpressing LDLR resulted in robust cell uptake, whereas PCSK9 uptake was very low in nontransfected cells (Fig. 4*C*). Both PCSK9 proline variants also displayed LDLR-dependent cell uptake (Fig. 4*C*), indicating that these proteins were not misfolded or otherwise grossly defective. In subsequent experiments, we focused on functional effects of the A44P mutation in PCSK9 because the methyl side chain of alanine is nonreactive and less likely to be directly involved in protein function.

Helical conformation specifically affects PCSK9 binding affinity to LDL

To more quantitatively assess the effect of the A44P mutation in full-length PCSK9, we performed a steady-state binding analysis in which fluorescent dye-labeled WT PCSK9 was incubated with LDL in the presence of increasing concentrations of unlabeled WT PCSK9 or PCSK9-A44P. For comparison purposes, we also included PCSK9 lacking the N-terminal 21 residues (Δ31–52), which is defective in LDL binding (18) and hyperactive in terms of LDLR binding/degradation (27, 34). Competition binding curves showed that the PCSK9-A44P mutant had a >5-fold decrease in LDL binding affinity compared with WT PCSK9 (Fig. 5, *A* and *B*), whereas Δ31–52-PCSK9 affinity for LDL was more than 2 orders of magnitude lower than that of WT PCSK9 (Fig. 5*A*). We also assessed the affinity of PCSK9-A44P for the purified LDLR extracellular domain (LDLR-ECD), which was decreased ~20% compared with WT PCSK9 (Fig. 5*C*). Nevertheless, when added to the medium of cultured HepG2 cells, PCSK9-A44P was able to mediate dose-dependent degradation of cell surface LDLRs at levels comparable with WT PCSK9 (Fig. 5*D*), in agreement with a recent study (29). Collectively, these data suggest that helical conformation in the prodomain N terminus plays a larger role in LDL binding relative to its role in PCSK9-LDLR association and LDLR degradation.

R46L substitution increases helix propensity in prodomain-derived peptides

The natural PCSK9 mutation R46L is a LOF variant associated with lowered plasma PCSK9 levels, an anti-atherogenic lipid profile and decreased incidence of CHD (5, 35, 36). Notably, an R46L substitution would extend the nonpolar face of the predicted AH motif in the IDR and reorient and increase the

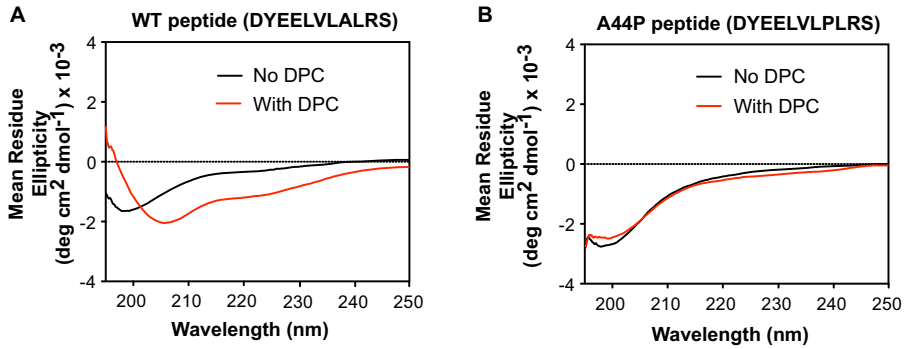

Figure 3. Amphipathic helix formation in the presence of a membrane mimetic. *A*, CD spectra of synthetic peptide representing WT PCSK9 residues 37–47 (DYEELVLALRS) in the absence (*black line*) or presence (*red line*) of DPC. Spectra shown are representative of three independent experiments. *B*, CD spectra obtained as in *A* using an A44P mutant peptide (DYEELVLPLRS).

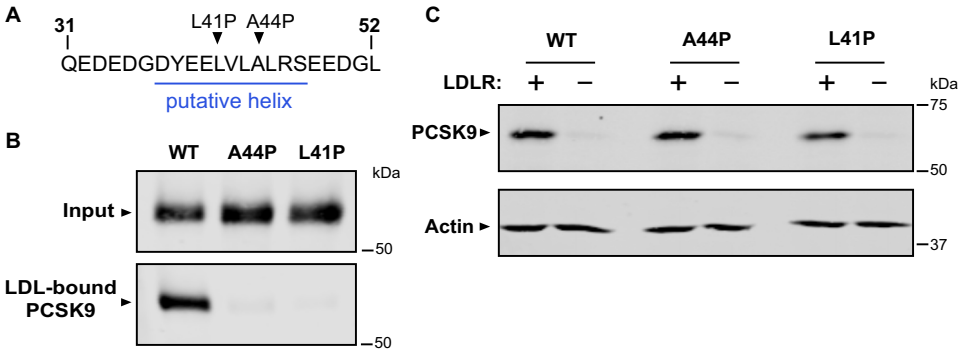

Figure 4. Proline substitutions in PCSK9 N terminus prevent LDL, but not LDLR, binding. *A*, position of proline substitutions in putative helical segment. *B*, analysis of *in vitro* PCSK9-LDL– binding reactions. Conditioned cell culture medium containing WT PCSK9 or proline mutants (A44P or L41P) were incubated with LDL prior to density gradient ultracentrifugation and Western blot analysis of LDL-containing fractions. *C*, HEK293 cells were transfected with LDLR (+) or vector control (−) and incubated with conditioned medium containing PCSK9 proteins. Cell uptake of PCSK9 was measured by Western blotting. Shown is a representative experiment ($n = 3$).

amplitude of the hydrophobic moment, as shown in helical wheel models (Fig. 6*A*). Helical net projections show the R46L mutation is also predicted to add additional side-chain interactions to stabilize the helical conformation (Fig. 6*B*). In agreement with these models, structural analysis using CD spectroscopy showed that an R46L-containing peptide representing residues 36–47 in PCSK9 presented a much stronger helical shift in a DPC micelle environment, with changes to both the intensity and position of the minimum relative to the corresponding WT peptide (Fig. 6*C*). The percent helicity of the peptides obtained at different DPC micelle concentrations allowed micelle binding curves to be obtained, revealing that the R46L substitution conferred an ~8-fold higher affinity for micelles compared with the WT peptide (Fig. 6, *D* and *E*). The R46L mutation in full-length PCSK9 did not affect binding affinity to isolated LDL particles, as unlabeled versions of WT PCSK9 and PCSK9-R46L showed nearly equal abilities to compete with dye-labeled PCSK9 for binding to LDL (Fig. S2).

Tyr-38 sulfation does not prevent PCSK9-LDL association

Numerous plasma proteins, such as exchangeable apolipoproteins, employ AH motifs for reversible binding to circulating lipoproteins (37). This function involves direct membrane association in which the nonpolar face of the helix intercalates between the fatty acyl chains in the single-layer phospholipid outer membrane of the lipoprotein. The transient AH in the PCSK9 prodomain has a comparatively small nonpolar face consisting of four residues, including Tyr-38 identified as a site of *O*-sulfation (38). We took advantage of this post-translational modification to test whether introduction of a negative sulfate group to the nonpolar face in the helix affected PCSK9's ability to bind LDL. HEK293 cells transiently overexpressing various PCSK9 constructs were incubated with Na-[^{35}S]O_4, and radiolabeled PCSK9 was immunoprecipitated for SDS-PAGE analysis. As previously reported (38), a PCSK9-Y38F variant was not ^{35}S-labeled, confirming Tyr-38 as the sole sulfation site in the prodomain under these experimental conditions (Fig. 7*A*). Following incubation with LDL, we were able to readily detect LDL-bound PCSK9 containing sulfated Tyr-38, whereas PCSK9-A44P containing sulfated Tyr-38 was defective in LDL binding (Fig. 7*B*). This result further suggests that helical structure in the prodomain N terminus is essential for LDL binding and also indicates that an uninterrupted hydrophobic face in the helix is not an absolute requirement. Nevertheless, hydrophobicity at this site could assist in formation of an AH motif in PCSK9 that facilitates LDL binding. In support of this hypothesis, hydrophobic substitutions (Y38F or Y38L) for the Tyr-38 residue were found to largely preserve LDL binding, whereas lower hydrophobicity (Y38A) caused a significant decrease of >50% (Fig. 7*C*). LDL binding was also decreased >60% by substitution of Tyr-38 with positively charged amino acids (Y38K or Y38R) but was less affected (decrease of ~25%) by substitution with acidic glutamic acid (Y38E) (Fig. 7*C*).

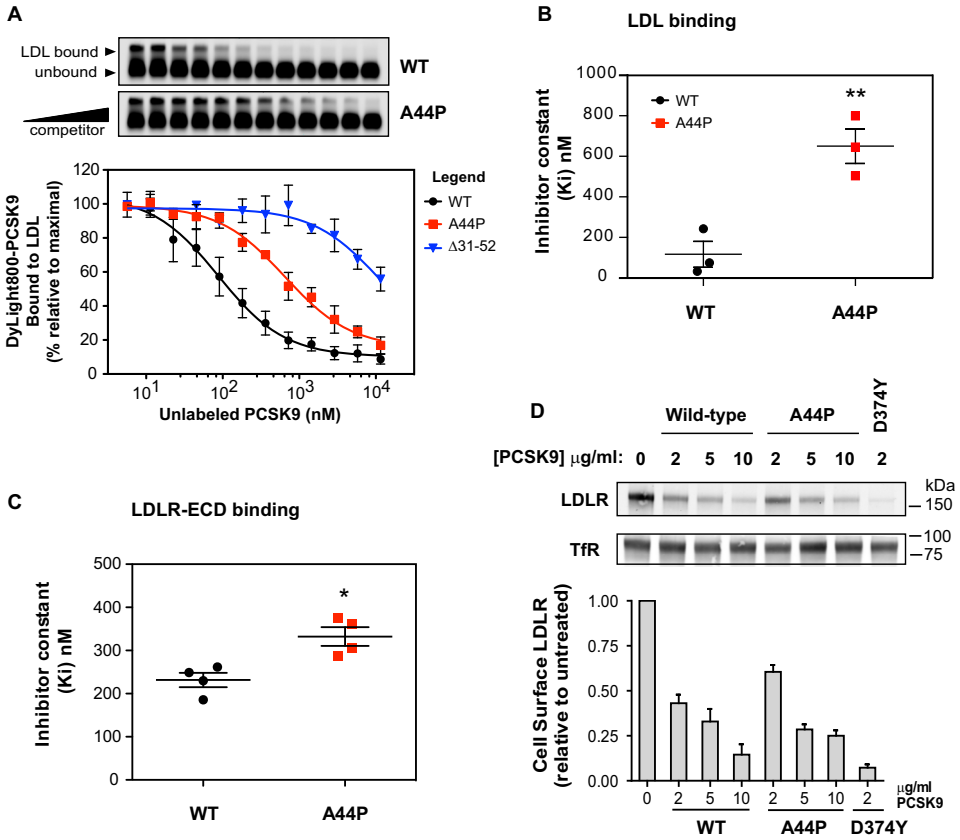

Figure 5. Helix-breaking A44P mutation in PCSK9 selectively inhibits LDL binding. *A*, *in vitro* competition binding of WT, A44P, and Δ31–52 forms of PCSK9 to LDL. LDL particles were incubated with Dylight800-labeled PCSK9 in the presence of increasing concentrations of unlabeled competitor proteins. Reaction mixtures were separated on agarose gels (*top*), and fluorophore-labeled PCSK9 binding to LDL was quantified and fitted to competition binding curves using nonlinear regression (*bottom*). *B*, inhibitor constants (K_i) obtained from *curves* in *A*. *Error bars*, S.E. ($n = 3$). Significant change in LDL binding of A44P mutant PCSK9 compared with WT PCSK9 was determined by Student's *t* test: **, $p < 0.01$. *C*, competition binding of WT PCSK9 and A44P mutant to LDLR-ECD. Shown is a *graphical representation* of inhibitor constants (K_i) obtained from binding curves. *Error bars*, S.E. ($n = 4$). Significant change in LDLR-ECD binding of A44P mutant PCSK9 compared with WT PCSK9 was determined by Student's *t* test: *, $p < 0.05$. *D*, dose response of cell surface LDLR degradation in HepG2 cells cultured 4 h in medium containing increasing concentrations of WT or A44P forms of PCSK9. Biotinylated cell surface LDLRs were isolated and quantified by Western blotting (*top*) using transferrin receptor (*TfR*) as a loading control. Densitometric data (*bottom*) were compared with untreated cells. LDLR degradation by GOF mutant D374Y PCSK9 was used for comparison and as a positive control. *Error bars*, S.E. ($n = 3$).

Evidence of an interdomain interaction required for PCSK9-LDL binding

The inability of Tyr-38 sulfation to prevent LDL binding (Fig. 7*B*) suggests that formation of the transient AH motif in the N-terminal region of PCSK9's prodomain promotes LDL association, although not necessarily through the membrane insertion of its hydrophobic face. Alternatively, the helical conformation could facilitate a protein-protein interaction, either directly with LDL-apoB100 or to an intramolecular site. To assess the latter possibility, computational molecular modeling of PCSK9 to include the missing IDR in known structures was performed using the *ab initio* structure prediction method implemented in ROSETTA (39, 40). Constraints from the highest-resolution PCSK9 X-ray crystal structure (PDB entry 2QTW) (26) were applied to conform to known parts of the protein, whereas an exhaustive conformational sampling was carried out to model residues 31–60. The resultant model in Fig. 8*A* shows the N-terminal prodomain inserted into a central cavity formed by the prodomain, the catalytic domain, and the CHR domain, stabilized in this position by an intramolecular interaction between an extended N-terminal helix (aa 32–48) and the CHR domain. The model also predicts adoption of helical conformation in a second sequence (aa 50–58) adjacent to a Ser-47 phosphorylation site (41) and within close proximity to a β-strand of the prodomain (denoted β_0) described as unique in PCSK9 compared with all known structures of subtilisin-like enzymes (11). The Arg-46 residue is located in an otherwise hydrophobic region of the N-terminal helix and does not interact with the rest of the protein; thus, it would be expected that the R46L LOF mutation in PCSK9 would expand a hydrophobic face of the helix. The intramolecular interaction predicted by our model involved negatively charged residues (Glu-32, Asp-35, and Glu-39) and aromatic Tyr-38 in the helical N-terminal prodomain conformation and multiple positively charged residues in the CHR domain (Arg-496, Arg-499, Arg-510, His-512, and His-565). Several GOF PCSK9 mutations associated with FH (R469W, R496W, and F515L) are clustered on a surface region of the CHR domain at or near the predicted interdomain interface (Fig. 8*A*, *inset*). When introduced into recombinant human PCSK9, all three mutations greatly inhibited LDL binding *in vitro* (Fig. 8, *B* and *C*). In particular, recombinant PCSK9-R496W appeared to be completely unable to bind LDL, whereas R469W and F515L substitutions lowered binding by ~60–70% (Fig. 8*C*). None of these mutations greatly affected PCSK9

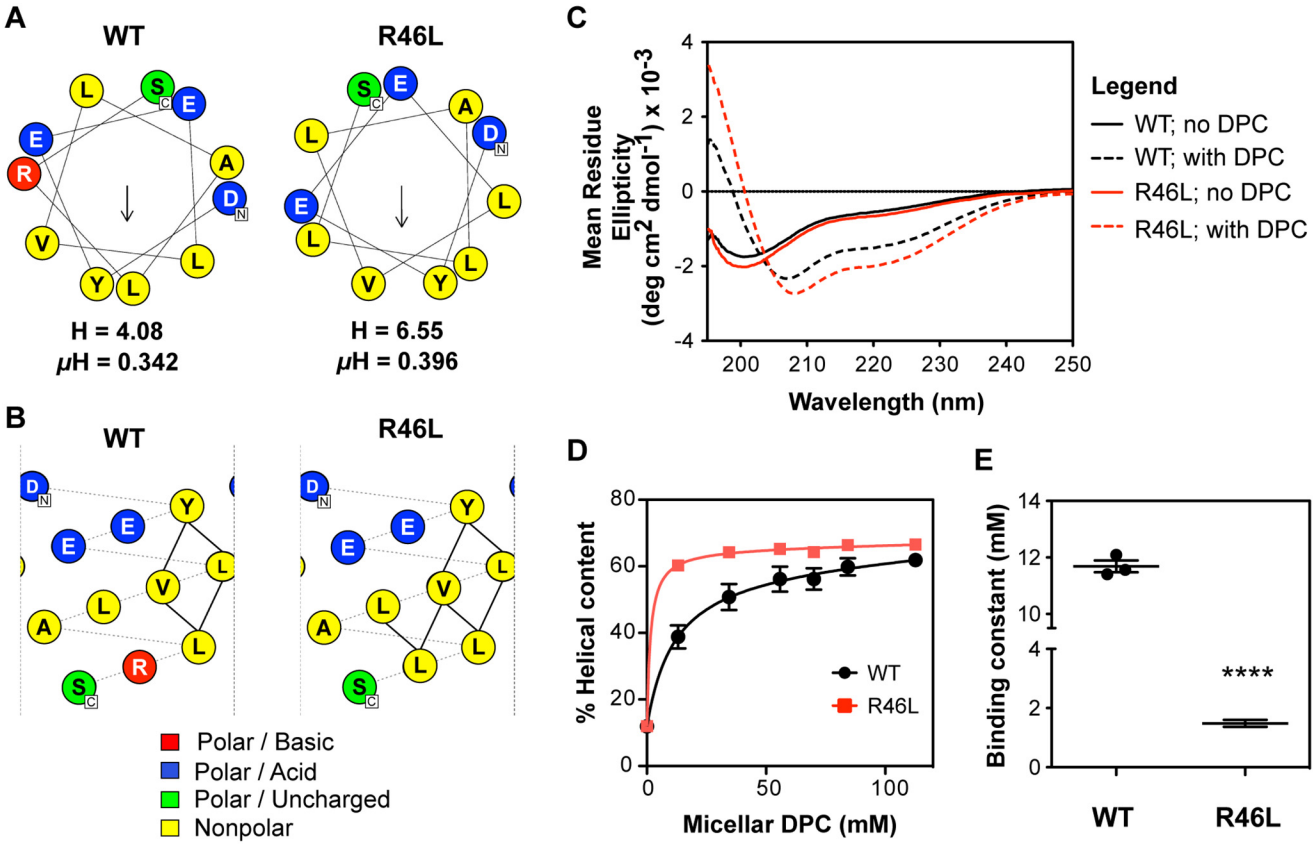

Figure 6. Natural mutation R46L modulates helicity in the prodomain N-terminal region. *A*, helical wheel representation of amphipathic α-helices (residues 37–47) generated from HeliQuest with either arginine or leucine at position 46. The *arrow* indicates the magnitude and direction of the hydrophobic moment (32). The hydrophobicity (*H*) and hydrophobic moment (*μH*) from HeliQuest are also shown. *B*, predicted hydrophobic side-chain interactions (*solid lines*) between residues of the putative N-terminal helix with either arginine or leucine at position 46. This was constructed on NetWheels software online (http://lbqp.unb.br/NetWheels/). (Please note that the JBC is not responsible for the long-term archiving and maintenance of this site or any other third party hosted site.) *C*, CD spectra prodomain peptides (either WT (GDYEELVLALRS) (*black*) or R46L (GDYEELVLALLS) (*red*)) in the absence (*solid lines*) or presence (*dashed lines*) of DPC micelles ($n = 3$). *D*, mean percentage helical content of either the WT or the R46L variant peptide as DPC concentration is increased. Secondary structure calculations were based on CD spectra using deconvolution algorithm CONTIN. *Error bars*, S.E. ($n = 3$). *E*, binding constants obtained from curves in *D*. *Error bars*, S.E. ($n = 3$). Significant change in micelle binding compared with WT peptide was determined by Student's *t* test: ****, $p < 0.0001$.

secretion into cell culture medium (data not shown), in agreement with a recent study (42), and all exhibited normal LDLR-dependent uptake in HEK293 cells (Fig. 8*D*). By contrast, a D374Y mutation known to increase LDLR binding affinity (2) clearly increased PCSK9 cell uptake (Fig. 8*D*). To further examine the effects of the R496W mutation, we purified secreted PCSK9-R496W protein (Fig. 8*E*) and found that it bound LDLR-ECD *in vitro* with similar affinity as WT PCSK9 (Fig. 8*F*) and also induced degradation of cell surface LDLRs with similar potency when added to the culture medium of HepG2 cells (Fig. 8*G*).

Discussion

IDRs in proteins frequently have crucial roles in regulatory and signaling processes due to increased flexibility and accessibility for post-translational modification and protein-protein interactions and in some cases undergo disorder-to-order structural transition as part of this function (43–45). We previously reported that association of PCSK9 with LDL particles *in vitro* depends on an IDR in the prodomain N terminus (18). In the current study, we provide biochemical, structural, and genetic evidence that this requirement is manifested as a transient AH, as follows: 1) an N-terminal prodomain-derived peptide adopted α-helical conformation in a membrane-mimetic environment (DPC micelles) (Fig. 3*A*), which was greatly enhanced by an R46L substitution representing an athero-protective *PCSK9* LOF mutation (Fig. 6); 2) a helix-breaking proline substitution (A44P) in PCSK9 lowered LDL binding affinity by >5-fold (Fig. 5, *A* and *B*); 3) a computational three-dimensional model of PCSK9 predicted that α-helical structure in prodomain N terminus aligns multiple polar residues to interact with the CHR domain (Fig. 8*A*); and 4) several *PCSK9* GOF mutations located at or near the predicted interface in the CHR domain greatly diminished LDL binding (Fig. 8*B*). Considered together, we propose a two-step process by which allosteric conformational changes in PCSK9 facilitate LDL binding: 1) the initial encounter with LDL in circulation provides lipid and/or protein contacts to trigger α-helix formation in the N-terminal IDR; 2) this structural transition aligns an interdomain interaction involving the prodomain and CHR domain, which in turn allows stable LDL association.

GOF mutations in *PCSK9* are rare in human populations and can result in substantially increased plasma LDL-C levels in FH patients (46). As such, delineation of underlying mechanisms can provide clear insight into aspects of PCSK9 function (6). As

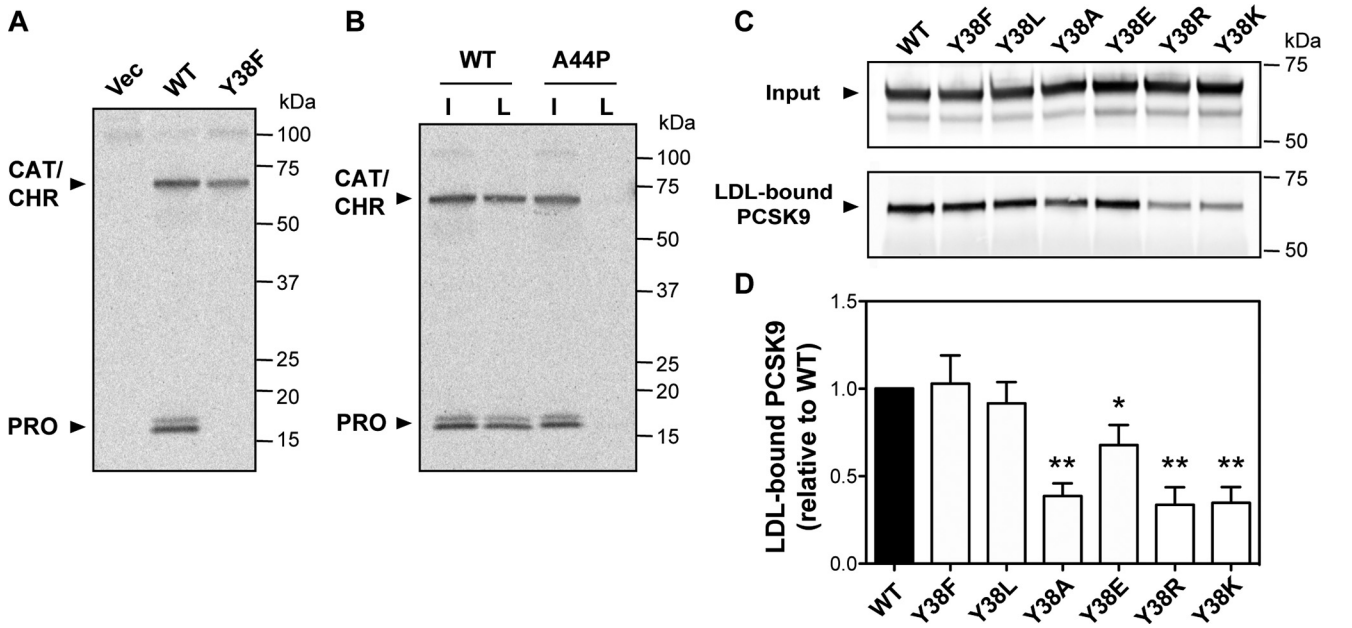

Figure 7. Role of amino acid position 38 (Tyr) in PCSK9-LDL binding. *A*, SDS-PAGE analysis of immunoprecipitated WT PCSK9 or Y38F mutant from conditioned medium of transiently transfected HEK293 radiolabeled with $[^{35}S]O_4$. In addition to sulfation of Tyr-38 in the ~16-kDa prodomain, the ~60-kDa catalytic domain/CHR domain segment is also labeled with $[^{35}S]O_4$ on a glycosyl moiety attached to Asn-544 (38). *B*, analysis of *in vitro* PCSK9-LDL– binding reactions. Conditioned medium containing ^{35}S-labeled WT PCSK9 or A44P mutant PCSK9 was incubated with LDL prior to density gradient ultracentrifugation to isolate an LDL fraction. *Lanes* are input (*I*) and LDL-bound PCSK9 (*L*). *C*, conditioned cell culture medium containing WT PCSK9 or the indicated Tyr-38 mutants were incubated with LDL prior to density gradient ultracentrifugation and Western blot analysis of LDL-containing fractions. *D*, densitometric analyses of Western blotting in *C*. *Error bars*, S.E. ($n = 4$). Significant change in LDL binding compared with WT PCSK9 control (set to 1.0) was determined by one-sample *t* test: *, $p < 0.05$; **, $p < 0.01$.

an example, the D374Y *PCSK9* mutation associated with severe hypercholesterolemia was found to greatly increase PCSK9-LDLR binding affinity and cellular LDLR degradation via an extracellular pathway, validating early *in vitro* evidence of the PCSK9-LDLR interaction (2). In Fig. 8*B*, we identify several GOF mutations in PCSK9 that severely inhibit (R469W and F515L) or abolish (R496W) LDL binding *in vitro*. The affected amino acids are clustered on a surface region in CHR domain module 1 (CM1) (aa 453–531), one of three structurally similar subdomains arranged in a pseudo-3-fold axis (26). This same site in CM1 was previously shown to engage a mAb that inhibited PCSK9-mediated LDLR degradation in cells and *in vivo* without affecting binding affinity to the LDLR EGF-A domain (47). Although the precise mechanism of PCSK9-LDL binding remains to be determined, Arg-496 could be a key residue in a prodomain-CM1 intramolecular interaction that serves as an essential component. In support, computational modeling studies predicted that adoption of helical conformation in the prodomain IDR aligns potential interactions between Asp-35, Tyr-38, and Glu-39 with Arg-496 in CM1 (Fig. 8*A*). The Arg-469 and Phe-515 residues do not interact with the prodomain in the model and possibly are more directly involved in binding to the LDL particle.

The R496W *PCSK9* mutation was first identified in an individual also heterozygous for an *LDLR* LOF mutation (E228K), the combined effect being severe hypercholesterolemia and early-onset cardiovascular heart disease (48). A high frequency of R496W *PCSK9* mutations (~9%) was recently reported in a Turkish FH cohort, associated with highly elevated plasma LDL-C levels and early onset CHD in seven of eight cases (49). In a multicenter study of FH associated with various *PCSK9* GOF mutations, the R496W mutation was among the more severe in terms of elevated LDL-C levels (46). Using purified PCSK9-R496W, we found that this mutant protein binds LDLR-ECD with normal affinity and induces cell surface LDLR degradation in cultured liver-derived cells to a similar extent as WT PCSK9 (Fig. 8, *F* and *G*). Like R496W, the R469W and F515L *PCSK9* mutations have been identified in FH patients (35, 50), but functional effects have remained unknown. In cell culture studies, all three GOF mutations exhibited only minor effects on maturation/secretion of PCSK9 and on LDLR-degrading ability (42, 51, 52). In the current study, LDLR-dependent uptake in HEK293 cells was largely unaffected (Fig. 8*D*). Given the lack of other functional effects, it is highly probable that defective LDL binding underlies the GOF phenotype associated with these *PCSK9* mutations in the CHR domain. Because PCSK9 activity raises plasma LDL levels, inhibition via direct binding to LDL particles could provide a form of negative feedback control. In this scenario, PCSK9 variants that bind poorly to LDL would be less subject to this inhibition, resulting in FH.

Lipid-ordered AHs are archetypal membrane-binding motifs found in numerous plasma proteins that, like PCSK9, reversibly associate with circulating lipoproteins and regulate lipoprotein metabolism (33, 37). However, the current data suggest that the primary function of a transient AH in PCSK9 is not membrane insertion, but rather alignment of an interdomain interaction that in turn facilitates LDL binding. This role in a protein-protein interaction is more akin to transient AH motifs found in acidic activation domains (AADs) of transcription factors. Most AADs are intrinsically disordered, which facilitates asso-

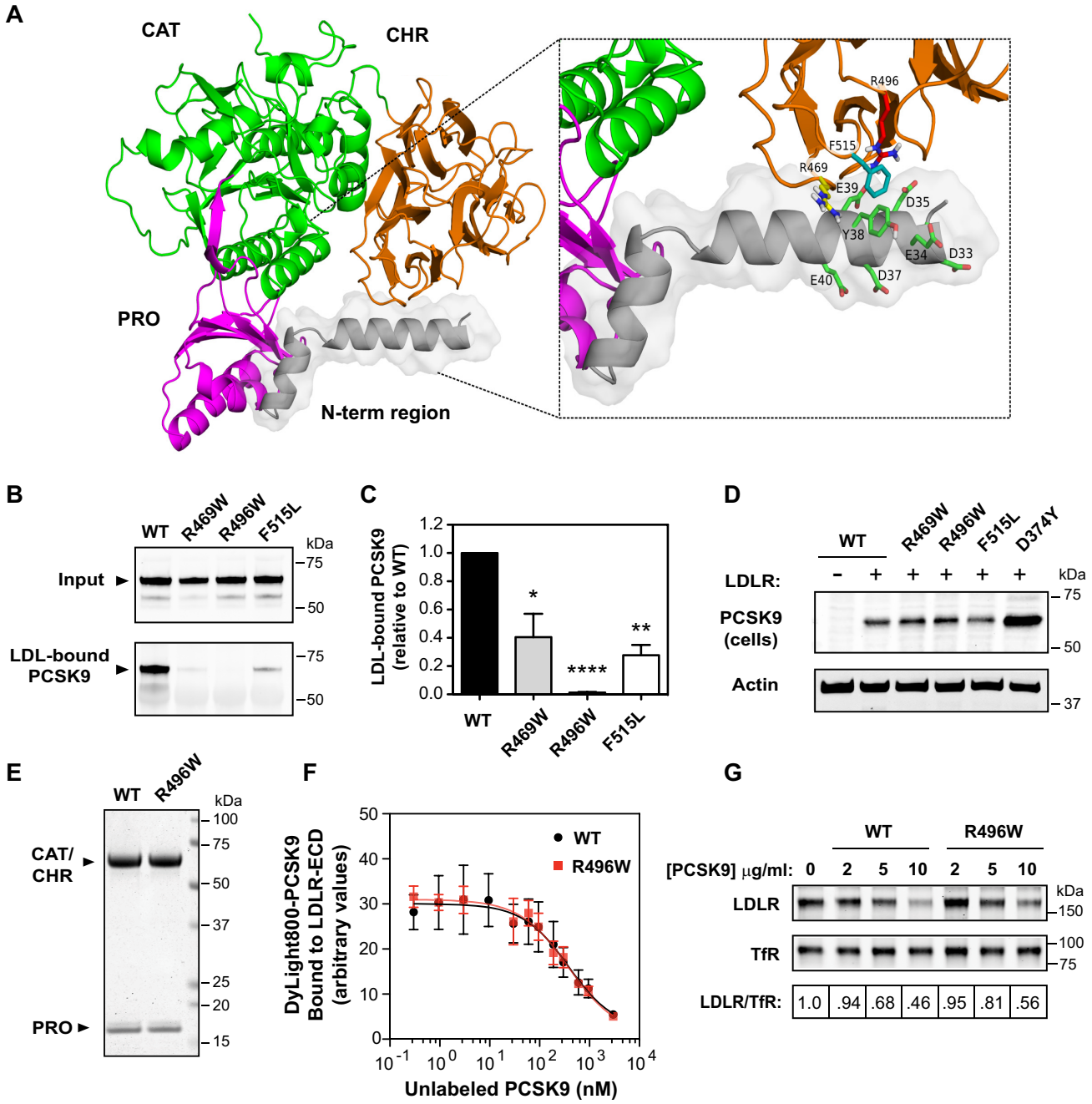

Figure 8. GOF *PCSK9* mutations in the C-terminal domain disrupt LDL binding *in vitro*. *A*, structure of full-length PCSK9 modeled by ROSETTA with constraints to conform to known parts of the structure from the highest-resolution X-ray crystal structure (PDB ID 2QTW) (26). The *color scheme* is as follows: prodomain (*Pro*, *magenta*), catalytic domain (*Cat*, *green*), CHR domain (*orange*), and N-terminal region of the prodomain (*gray* with *transparent surfaces*). *Box*, details of prodomain/CHR domain interface. *Side-chain sticks* (*green*) highlight polar residues in the N-terminal region; *side-chain sticks* for Arg-469 (*yellow*), Arg-496 (*red*), and Phe-515 (*cyan*) show the close proximity of residues associated with FH. *B*, analysis of *in vitro* PCSK9-LDL– binding reactions. Conditioned medium containing WT PCSK9 or GOF variants R469W, R496W, and F515L was incubated with LDL prior to density gradient ultracentrifugation to isolate an LDL fraction and visualization of PCSK9 by Western blotting. *C*, densitometric analyses of Western blotting in *C*. *Error bars*, S.E. ($n = 4$). Significant change in LDL binding compared with WT PCSK9 control (set to 100%) was determined by one-sample *t* test: *, $p < 0.05$; **, $p < 0.01$; ****, $p < 0.0001$. *D*, HEK293 cells were transfected with LDLR (+) or vector control (−) and incubated with conditioned medium containing the indicated PCSK9 proteins. Cell uptake of PCSK9 was visualized by Western blotting. Shown is a representative experiment ($n = 3$). *E*, Coomassie staining of SDS-polyacrylamide gel separation of purified WT and R496W PCSK9 proteins. *F*, competition binding of WT PCSK9 and R496W mutant to LDLR-ECD ($n = 3$). *G*, dose response of cell surface LDLR degradation in HepG2 cells cultured 4 h in medium containing increasing concentrations of WT or R496W forms of PCSK9. Biotinylated cell surface LDLRs were isolated and quantified by Western blotting using transferrin receptor (*TfR*) as a loading control. Shown is a representative experiment ($n = 3$).

ciation with multiple partner proteins in an amorphous and flexible manner (53). In some cases, coupled folding and binding occurs driven by weak hydrophobic "encounter" interactions that initiate helix formation (54). A paradigm for the evolution of transient helical motifs in signaling proteins of higher organisms is the tumor suppressor p53, in which formation of short AH interaction motifs in its AAD modulates target protein binding and transcriptional control (55–57). In a similar manner, order/disorder transition in the acidic prodomain IDR of PCSK9 could affect the stringency or affinity of its interac-

tions with potential binding partners, including other intramolecular sites.

A previous study showed that PCSK9 lacking an N-terminal portion of the prodomain IDR (Δ31–52) bound LDLR *in vitro* with >7-fold higher affinity, identifying a negative allosteric function (27). Further studies narrowed this effect to a highly acidic segment (aa 32–40; EDEDGDYEE) hypothesized to participate in intramolecular electrostatic interactions in a cryptic autoinhibited conformation, perhaps involving the CHR domain (28, 30, 58). Indeed, a predicted interdomain interface site in CM1 (Fig. 8*A*) contains a cluster of arginine residues at positions 469, 496, 499, and 510 that could interact with acidic amino acids in a disordered prodomain N terminus. This may be sufficient to maintain PCSK9 in an autoinhibited state under basal conditions, explaining why a helix-breaking A44P mutation in PCSK9 did not increase LDLR binding/degradative functions (Fig. 5, *C* and *D*). On the other hand, adoption of rigid α-helical structure could favor certain contacts, possibly involving the Arg-496 residue identified as key to LDL binding (Fig. 8*B*). If so, this would explain why PCSK9-A44P had lowered LDL binding affinity but was not as defective in this function as Δ31–52-PCSK9, in which an interaction with CM1 would be completely abolished (Fig. 5, *A* and *B*). Indeed, LDL association may stabilize an autoinhibitory prodomain-CM1 interaction in PCSK9 that otherwise can be released by activating factors. Two such factors are known to improve the LDLR-binding function of PCSK9, namely acidic pH (11, 16, 22) and its association with heparin sulfate proteoglycans at the surface of hepatocytes (59). Heparin sulfate proteoglycans were recently shown to modulate the ability of LDL to inhibit PCSK9 activity, suggesting an interplay between these regulatory factors (23).

The N-terminal prodomain IDR is the site of several *PCSK9* mutations associated with plasma LDL-C levels in humans (6, 28), including an atheroprotective R46L *PCSK9* allele found in ~3% of Caucasians (5, 36, 60). Unlike more deleterious LOF mutations that disrupt autocatalytic cleavage or protein folding, R46L does not affect PCSK9 secretion (61), and only minor effects of this mutation on cellular LDLR binding and degradation have been reported (22, 58, 62). As shown in Fig. 6, this mutation is predicted to extend the hydrophobic face of a transient AH motif, and an R46L substitution in a prodomain-derived peptide had a substantial positive effect on coil-to-helix structural transition in the presence of DPC micelles, a membrane mimetic. Thus, increased helix propensity could contribute to the LOF phenotype, perhaps via enhanced plasma clearance of PCSK9-R46L as a passive component of LDL particles. In support, individuals carrying the R46L allele have significantly lowered plasma PCSK9 concentrations (35). Counter to this hypothesis, we found that purified recombinant PCSK9-R46L displayed normal LDL binding affinity *in vitro* (Fig. S2). However, it should be noted that the *PCSK9* R46L allele in humans is associated with only modest lowering of plasma LDL-C (~15%) with athero-protection likely due to life-long exposure (5, 60). Thus, it is predictable that any acute functional effects of R46L in full-length PCSK9 will be slight, highlighting the utility of structural approaches for mechanistic insight.

The prodomain IDR is also the site of two post-translational modifications, namely phosphorylation at Ser-47 (41) and sulfation at Tyr-38 (38). Although Tyr-38 sulfation introduces a negative charge within the hydrophobic face of the transient AH motif (Fig. 2*D*), it did not affect LDL binding *in vitro* (Fig. 7*B*). On the other hand, mutation of Tyr-38 to alanine lowered PCSK9-LDL binding by >50%, whereas substitutions of higher hydrophobicity (Phe or Leu) preserved LDL binding (Fig. 7, *C* and *D*). A possible explanation is that decreased hydrophobicity upon Tyr-38 sulfation is compensated by direct involvement of the sulfotyrosine residue in the prodomain-CM1 interaction that controls LDL binding. In a recent study, a mAb was shown to specifically bind and stabilize helical conformation in peptides derived from the N-terminal IDR in the PCSK9 prodomain (29). Binding affinity was greatly enhanced by sulfation of Tyr-38 (29), consistent with a known role of sulfotyrosine in promoting protein-protein interactions (63, 64). Post-translational modifications often modulate the functional interactions of short interaction motifs within IDRs in proteins (65); thus, Tyr-38 sulfation could serve this role in the N-terminal prodomain IDR in PCSK9.

Determining the functional outcome of PCSK9-LDL binding is crucial to our overall understanding of reciprocal feedback mechanisms that control plasma concentrations of LDL-C and associated risk of cardiovascular heart disease. It is established that LDLR-mediated uptake and degradation of LDL particles in hepatocytes raises intracellular levels of cholesterol and suppresses activity of the SREBP-2 transcription factor, thereby lowering gene expression of both LDLR and PCSK9 (3, 66). Also, LDLR-mediated uptake of PCSK9 results in LDLR degradation and reduced LDL and PCSK9 clearance from plasma (13). The data in the current study support the existence of an additional feedback loop whereby circulating PCSK9 activity is inhibited via its direct interaction with LDL particles in response to intravascular LDL accumulation. The identification of point mutant forms of PCSK9 selectively defective for LDL association, such as A44P, provides important molecular tools to further test this hypothesis in animal models of dyslipidemia.

Experimental procedures

Materials

We obtained fetal bovine serum and newborn calf serum from Thermo Fisher Scientific and Optiprep™ density gradient medium (60% (w/v) iodixanol) from Axis-Shield. EDTA-free Complete™ protease inhibitor tablets were from Roche Applied Science, Nonidet P-40 detergent was from Biovision, and PolyJet DNA transfection reagent was from FroggaBio (Toronto, Canada). All other reagents were from Sigma-Aldrich unless otherwise specified. Sodium mevalonate was prepared from mevalonic acid as described (67). Newborn calf lipoprotein-deficient serum (NCLPDS) ($d > 1.215$ g/ml) was prepared by ultracentrifugation (68). The LDLR cDNA expression vector used in these studies was pLDLR17 (69).

Cell culture

HEK293 and HepG2 cells (American Type Culture Collection) were maintained in monolayer culture at 37 °C and 5%

CO_2 in one of the following media. Medium A contained Dulbecco's modified Eagle's medium (4.5 g/liter glucose; Gibco) supplemented with 100 units/ml penicillin and 100 μg/ml streptomycin sulfate; Medium B contained Medium A supplemented with 10% fetal bovine serum (v/v); Medium C contained Medium A supplemented with 5% (v/v) NCLPDS; Medium D contained Dulbecco's modified Eagle's medium (1.0 g/liter glucose; Gibco) supplemented with 100 units/ml penicillin and 100 μg/ml streptomycin sulfate; sterol-depleting Medium E contained Medium D supplemented with 5% (v/v) NCLPDS, 10 μM pravastatin, and 50 μM sodium mevalonate.

Protein purification and labeling

FLAG epitope-tagged recombinant human WT PCSK9 along with A44P, R46L, R496W, and Δ31–52 variants were produced in stably transfected HEK293S cells and purified from conditioned culture medium as described previously (18). Fluorescently labeled WT PCSK9 was prepared using the DyLight800 antibody-labeling kit (Thermo Fisher Scientific) as per the manufacturer's instructions followed by gel filtration chromatography on a Superdex 200 10/300 GL column (GE Healthcare) to remove unbound dye. The extracellular domain (ECD) of LDLR used for PCSK9 binding assays was partially purified from conditioned medium of HEK293S cells cultured as described (18) stably transfected with a plasmid encoding amino acids 1–692 of human LDLR containing a C-terminal His_6 tag (a kind gift from R. Milne, University of Ottawa). LDLR-ECD was enriched by affinity chromatography using TALON superflow affinity resin (Clontech) followed by gel filtration chromatography on a Superdex 200 10/300 GL column (GE Healthcare).

Antibodies

The following antibodies were used for Western blotting. A mouse hybridoma clone expressing mAb 15A6 recognizing an epitope in the C-terminal CHR domain of PCSK9 was a generous gift from J. Horton (University of Texas Southwestern Medical Center, Dallas, TX). The IgG fraction was purified from hybridoma culture medium by Protein A chromatography on a Profinia™ protein purification system (Bio-Rad) as per the manufacturer's instructions. Rabbit antiserum 3143 against the C-terminal 14 amino acids of LDLR was a kind gift of J. Herz (University of Texas Southwestern Medical Center). Anti-actin mouse monoclonal ascites fluid (clone AC-40) was from Sigma. The mouse anti-human transferrin receptor antibody was from Life Technologies, Inc. Secondary IRDye-labeled goat anti-mouse and anti-rabbit IgG antibodies were from LI-COR Biosciences. Rabbit antiserum 1697 raised against full-length human PCSK9 was used for immunoprecipitation and was custom-produced by Biomatik (Cambridge, Canada).

Western blotting

Samples were loaded onto 8% SDS-polyacrylamide gels or 4–12% Tris/HEPES-SDS Bolt™ precast gels (Thermo-Invitrogen) for electrophoresis. The size-separated proteins were then transferred to nitrocellulose membranes (Bio-Rad). Primary antibodies (described above) and IRdye800-conjugated secondary antibodies were used to detect target proteins. Signal was detected using the LI-COR Odyssey IR imaging system (LI-COR Biosciences). Quantification of the intensity of the bands was obtained using Odyssey 2.0 software (LI-COR Biosciences).

Site-directed mutagenesis

The pcDNA3-PCSK9-FLAG vector (70) codes for full-length human WT PCSK9 with a FLAG tag epitope attached at the C terminus. This vector was used as the template to generate PCSK9 mutants. Mutagenesis was carried out using the QuikChange site-directed mutagenesis protocol from Stratagene (La Jolla, CA). PCR primers were custom-synthesized by Invitrogen-Life Technologies or Integrated DNA Technologies. The primers used for generation of the mutants are listed in Table S1. All desired mutations and the absence of extraneous mutations were confirmed by sequencing the entire coding region.

Preparation of conditioned media

HEK293 cells cultured in Medium B to ~70% confluence in a 100-mm Petri dish were transfected with a total of 3 μg of PCSK9 cDNA expression vectors using PolyJet DNA transfection reagent as per the manufacturer's instructions. At 18 h post-transfection, the cells were washed and incubated with serum-free Medium A containing 1× ITS (insulin-transferrin-selenium) cell culture supplement. Conditioned media were recovered 48 h post-transfection and buffer-exchanged with HBS-C (HEPES-buffered saline-calcium buffer: 25 mM HEPES-KOH, pH 7.4, 150 mM NaCl, 2 mM $CaCl_2$) and concentrated ~10-fold on an Amicon Ultra-4 centrifugal filter unit with a 10-kDa membrane cutoff (Millipore). PCSK9 in conditioned medium preparations was quantified by Western blot analysis using purified PCSK9 as a standard and stored in single-use aliquots at −80 °C.

LDL isolation

All procedures using human subjects received regulatory approval from the Human Research Ethics board at the University of Ottawa Heart Institute and abide by the Declaration of Helsinki principles. Blood samples were drawn from fasted healthy volunteers into evacuated tubes containing EDTA, and plasma was separated by low-speed centrifugation. Protease inhibitors (1 mM phenylmethylsulfonyl fluoride, 50 units/ml aprotinin, and Complete™ protease inhibitor mixture) and antioxidant (20 μM butylated hydroxytoluene) were added to the cleared plasma. LDL (d = 1.019–1.065 g/ml) was isolated using sequential potassium bromide flotation ultracentrifugation (71) followed by extensive dialysis against PBS containing 0.25 mM EDTA. LDL was stored at 4 °C protected from light and used within 2–3 weeks. Alternatively, LDL was stored at −80 °C in 10% (w/v) sucrose as described (72), which did not affect subsequent PCSK9-binding tests.

PCSK9-LDL binding assay

Binding reactions (1.0-ml volume), each containing 500 μg of LDL and 1 μg of PCSK9 (in concentrated conditioned media) and 0.5% BSA (w/v) in HBS-C buffer (25 mM HEPES-KOH, pH 7.4, 150 mM NaCl, 2 mM $CaCl_2$) were incubated at 37 °C for 1 h.

LDL-bound and free PCSK9 were then separated by Optiprep gradient ultracentrifugation according to a modified version of a protocol described previously (73). Briefly, a 9% Optiprep sample solution was prepared by diluting 1.0 ml of each binding reaction with 0.45 ml of 60% Optiprep and 1.55 ml of 25 mM HEPES-KOH, pH 7.4. The 9% sample was overlaid with 25 mM HEPES-KOH, pH 7.4, in a 3.3-ml Optiseal tube (Beckman). Tubes were centrifuged in a TLN100 rotor (Beckman Coulter) at 100,000 rpm for 2 h at 4 °C. LDL-containing fractions (600 μl) were collected by tube puncture into a 1-ml syringe. The entire LDL fraction was immunoprecipitated for 18 h at 4 °C using anti-PCSK9 rabbit polyclonal 1697 (see above) and anti-rabbit Trueblot agarose beads (Rockland). The collected beads were washed, and immunoprecipitated proteins were resolved by SDS-PAGE on 8% acrylamide gels. PCSK9 content was then quantified by Western blotting, and values were normalized to reactions containing WT PCSK9.

Competition binding curves

For PCSK9-LDL binding analysis, 0.5 mg/ml LDL was incubated with 10 nM DyLight800-labeled WT PCSK9 in HBS-C buffer containing 1% (w/v) BSA for 90 min at 37 °C with increasing amounts of unlabeled WT or mutant PCSK9. 4× loading dye (10% Ficoll-400, 0.01% bromphenol blue) was added to the reactions, and the mixtures were resolved on 0.7% agarose gels (SeaKem LE) for 2 h at 40 V with electrode buffer of 90 mM Tris, pH 8.0, 80 mM borate, 2 mM calcium lactate. Gels were scanned directly using the LI-COR Odyssey IR imaging system (LI-COR Biosciences), and bands representing DyLight800-PCSK9 bound to LDL were quantified using Odyssey 2.0 software (LI-COR Biosciences). For PCSK9-LDLR binding analysis, partially purified LDLR-ECD (see above) was diluted in TBS-C (50 mM Tris, pH 7.4, 90 mM NaCl, 2 mM $CaCl_2$) and blotted directly onto 0.45-μm pore size nitrocellulose membranes (Bio-Rad) using a BioDot SP slot-blot apparatus (Bio-Rad) according to the manufacturer's instructions, and blots were blocked for 30 min in TBS-C containing 5% (w/v) nonfat milk. All incubations (90 min) and subsequent washes (3 × 15 min) were carried out at room temperature with gentle oscillation in TBS-C buffer containing 2.5% (w/v) nonfat milk. Blots were incubated with 0.1 μg/ml DyLight800-labeled WT PCSK9 with increasing amounts of unlabeled WT or mutant PCSK9. Blots were then washed and scanned using the LI-COR Odyssey IR Imaging System, and band intensity was quantified using Odyssey version 2.0 software (LI-COR Biosciences). The amount of competitor PCSK9 protein required for 50% inhibition of fluorophore-labeled PCSK9 binding (K_i) was determined by fitting data to a sigmoidal dose-response curve using nonlinear regression (GraphPad Prism 5 software).

PCSK9 cellular uptake assays

HEK293 cells were cultured in Medium B in 6-well dishes to 70% confluence and then transiently transfected with 1 μg of WT human LDLR plasmid per well using PolyJet DNA transfection reagent as per the manufacturer's instructions. The following day, cells were switched to lipoprotein-deficient Medium C and treated for 2 h at 37 °C with 2 μg/ml PCSK9 (from conditioned media) in the presence of 50 μM chloroquine. Cells were then washed in ice-cold PBS-CM (PBS with 1 mM $MgCl_2$ and 0.1 mM $CaCl_2$), and whole-cell extracts were prepared in Tris Lysis Buffer (50 mM Tris-Cl, pH 7.4, 150 mM NaCl, 1% Nonidet P-40, 0.5% sodium deoxycholate, 5 mM EDTA, 5 mM EGTA, 1× Complete™ protease inhibitor mixture, 1 mM phenylmethylsulfonyl fluoride). Extracted proteins were resolved on 8% SDS-PAGE, and LDLR, PCSK9 and actin were detected by Western blotting.

Cell surface LDLR degradation assays

HepG2 cells in 60 mM dishes were cultured in Medium D to 60% confluence and then switched to sterol-depleting Medium E for 18–20 h. Purified, recombinant WT or A44P- or D374Y-PCSK9 was added to the medium, and cells were incubated at 37 °C for 4 h. Cell surface proteins were biotinylated with Sulfo-NHS-SS-Biotin (Campbell Science, Rockford, IL) and captured from whole-cell extracts using NeutrAvidin-agarose beads (Pierce) as described previously (74). Biotinylated proteins were eluted by boiling in sample buffer supplemented with 5% β-mercaptoethanol, and proteins were resolved on 8% SDS-PAGE and immunoblotted for LDLR and transferrin receptor.

Circular dichroism

Custom peptide synthesis (>98% purity) was by BioMatik. Lyophilized peptides were initially dissolved as stock solutions in 0.1% ammonium hydroxide, and peptide concentrations were determined by amino acid analysis (SPARC BioCentre, University of Toronto) for use in mean residue molar ellipticity calculations. CD spectra were collected on 30 μM samples of peptides in 10 mM Tris, pH 8.5, and 130 mM NaCl with or without 2.5% (w/v) DPC micelles using a Jasco J-815 CD spectropolarimeter at 37 °C with a 0.1-cm quartz cuvette. Spectra were acquired from 200 to 250 nm using five accumulations at 20 nm/min and a data integration time of 8 s. Secondary structure deconvolution of spectra was carried out in CDPro with the CONTIN algorithm and SP43 reference set. To measure the apparent affinity of peptide-lipid interactions, peptide (30 μM) was mixed with increasing concentrations of DPC micelles, and CD spectra were collected after each increment as described above.

Modeling of the PCSK9 N-terminal prodomain

The crystal structure of PCSK9 at 1.9 Å resolution (PDB entry 2QTW) (26) was used to model the missing residues in the N-terminal region of the prodomain. The structure adopted by residues 31–60 was built employing the fragment-based *de novo* protein structure prediction method implemented in ROSETTA version 3.8 (40). In preparation for the modeling, 3-mer and 9-mer fragment library files were created with the ROBETTA server (39), identifying protein fragment structures in the Protein Data Bank that are compatible with the PCSK9 sequence. Based on these libraries, 180,000 refined PCSK9 models including the N-terminal prodomain were built. The known part of the PCSK9 structure was kept fixed during the conformational search. Analysis of the ROSETTA total score against the Cα root mean square deviation relative to the lowest-score model was used to evaluate the modeling convergence. The best full-length PCSK9 model was selected as that

with the lowest ROSETTA score. Secondary structure prediction with PSIPRED version 3.3 (75) as well as protein compactness and local secondary structural features estimated with the "protein meta-structure" approach (76) are consistent with the predicted structure. The final model was analyzed using PyMOL version 1.8.4 (Schrödinger, LLC, New York).

Statistics

Data are presented as the mean ± S.E. Two-sided statistical analysis was determined by one-sample *t* test or Student's *t* test, as indicated in the figure legends, using GraphPad Prism 5 software. Data used measurements from at least two distinct sample preparations for each component.

Author contributions—S. K. S., A. C. F., A. M., T. K., A. V.-J., and T. A. L. data curation; S. K. S., A. C. F., A. M., N. K. G., A. V.-J., and T. A. L. formal analysis; S. K. S., A. C. F., I. A., N. K. G., A. V.-J., and T. A. L. investigation; S. K. S., A. C. F., A. M., T. K., N. K. G., A. V.-J., and T. A. L. methodology; S. K. S., A. C. F., A. M., T. K., N. K. G., A. V.-J., and T. A. L. writing-review and editing; N. K. G. and T. A. L. supervision; A. V.-J. and T. A. L. conceptualization; A. V.-J. and T. A. L. resources; A. V.-J. and T. A. L. funding acquisition; T. A. L. validation; T. A. L. visualization; T. A. L. writing-original draft; T. A. L. project administration.

References

1. Maxwell, K. N., and Breslow, J. L. (2004) Adenoviral-mediated expression of Pcsk9 in mice results in a low-density lipoprotein receptor knockout phenotype. *Proc. Natl. Acad. Sci. U.S.A.* **101,** 7100–7105 CrossRef Medline
2. Lagace, T. A., Curtis, D. E., Garuti, R., McNutt, M. C., Park, S. W., Prather, H. B., Anderson, N. N., Ho, Y. K., Hammer, R. E., and Horton, J. D. (2006) Secreted PCSK9 decreases the number of LDL receptors in hepatocytes and in livers of parabiotic mice. *J. Clin. Invest.* **116,** 2995–3005 CrossRef Medline
3. Horton, J. D., Cohen, J. C., and Hobbs, H. H. (2009) PCSK9: a convertase that coordinates LDL catabolism. *J. Lipid Res.* **50**, S172–S177 CrossRef Medline
4. Abifadel, M., Varret, M., Rabès, J. P., Allard, D., Ouguerram, K., Devillers, M., Cruaud, C., Benjannet, S., Wickham, L., Erlich, D., Derré, A., Villéger, L., Farnier, M., Beucler, I., Bruckert, E., *et al.* (2003) Mutations in *PCSK9* cause autosomal dominant hypercholesterolemia. *Nat. Genet.* **34,** 154–156 CrossRef Medline
5. Cohen, J. C., Boerwinkle, E., Mosley, T. H., Jr., and Hobbs, H. H. (2006) Sequence variations in PCSK9, low LDL, and protection against coronary heart disease. *N. Engl. J. Med.* **354,** 1264–1272 CrossRef Medline
6. El Khoury, P., Elbitar, S., Ghaleb, Y., Khalil, Y. A., Varret, M., Boileau, C., and Abifadel, M. (2017) PCSK9 mutations in familial hypercholesterolemia: from a groundbreaking discovery to anti-PCSK9 therapies. *Curr. Atheroscler. Rep.* **19,** 49 CrossRef Medline
7. Stein, E. A., and Raal, F. J. (2013) Insights into PCSK9, low-density lipoprotein receptor, and low-density lipoprotein cholesterol metabolism: of mice and man. *Circulation* **127,** 2372–2374 CrossRef Medline
8. Stein, E. A., and Raal, F. (2014) Reduction of low-density lipoprotein cholesterol by monoclonal antibody inhibition of PCSK9. *Annu. Rev. Med.* **65,** 417–431 CrossRef Medline
9. Seidah, N. G., Sadr, M. S., Chrétien, M., and Mbikay, M. (2013) The multifaceted proprotein convertases: their unique, redundant, complementary, and opposite functions. *J. Biol. Chem.* **288,** 21473–21481 CrossRef Medline
10. Benjannet, S., Rhainds, D., Essalmani, R., Mayne, J., Wickham, L., Jin, W., Asselin, M. C., Hamelin, J., Varret, M., Allard, D., Trillard, M., Abifadel, M., Tebon, A., Attie, A. D., Rader, D. J., *et al.* (2004) NARC-1/PCSK9 and its natural mutants: zymogen cleavage and effects on the low density lipoprotein (LDL) receptor and LDL cholesterol. *J. Biol. Chem.* **279,** 48865–48875 CrossRef Medline
11. Cunningham, D., Danley, D. E., Geoghegan, K. F., Griffor, M. C., Hawkins, J. L., Subashi, T. A., Varghese, A. H., Ammirati, M. J., Culp, J. S., Hoth, L. R., Mansour, M. N., McGrath, K. M., Seddon, A. P., Shenolikar, S., Stutzman-Engwall, K. J., *et al.* (2007) Structural and biophysical studies of PCSK9 and its mutants linked to familial hypercholesterolemia. *Nat. Struct. Mol. Biol.* **14,** 413–419 CrossRef Medline
12. Grefhorst, A., McNutt, M. C., Lagace, T. A., and Horton, J. D. (2008) Plasma PCSK9 preferentially reduces liver LDL receptors in mice. *J. Lipid Res.* **49,** 1303–1311 CrossRef Medline
13. Tavori, H., Fan, D., Blakemore, J. L., Yancey, P. G., Ding, L., Linton, M. F., and Fazio, S. (2013) Serum proprotein convertase subtilisin/kexin type 9 and cell surface low-density lipoprotein receptor: evidence for a reciprocal regulation. *Circulation* **127,** 2403–2413 CrossRef Medline
14. Rudenko, G., Henry, L., Henderson, K., Ichtchenko, K., Brown, M. S., Goldstein, J. L., and Deisenhofer, J. (2002) Structure of the LDL receptor extracellular domain at endosomal pH. *Science* **298,** 2353–2358 CrossRef Medline
15. Beglova, N., Jeon, H., Fisher, C., and Blacklow, S. C. (2004) Cooperation between fixed and low pH-inducible interfaces controls lipoprotein release by the LDL receptor. *Mol. Cell* **16,** 281–292 CrossRef Medline
16. Zhang, D.-W., Lagace, T. A., Garuti, R., Zhao, Z., McDonald, M., Horton, J. D., Cohen, J. C., and Hobbs, H. H. (2007) Binding of proprotein convertase subtilisin/kexin type 9 to epidermal growth factor-like repeat A of low density lipoprotein receptor decreases receptor recycling and increases degradation. *J. Biol. Chem.* **282,** 18602–18612 CrossRef Medline
17. Zhang, D. W., Garuti, R., Tang, W. J., Cohen, J. C., and Hobbs, H. H. (2008) Structural requirements for PCSK9-mediated degradation of the low-density lipoprotein receptor. *Proc. Natl. Acad. Sci. U.S.A.* **105,** 13045–13050 CrossRef Medline
18. Kosenko, T., Golder, M., Leblond, G., Weng, W., and Lagace, T. A. (2013) Low density lipoprotein binds to proprotein convertase subtilisin/kexin type-9 (PCSK9) in human plasma and inhibits PCSK9-mediated low density lipoprotein receptor degradation. *J. Biol. Chem.* **288,** 8279–8288 CrossRef Medline
19. Hori, M., Ishihara, M., Yuasa, Y., Makino, H., Yanagi, K., Tamanaha, T., Kishimoto, I., Kujiraoka, T., Hattori, H., and Harada-Shiba, M. (2015) Removal of plasma mature and furin-cleaved proprotein convertase subtilisin/kexin 9 by low-density lipoprotein-apheresis in familial hypercholesterolemia: development and application of a new assay for PCSK9. *J. Clin. Endocrinol. Metab.* **100,** E41–E49 CrossRef Medline
20. Sun, H., Samarghandi, A., Zhang, N., Yao, Z., Xiong, M., and Teng, B. B. (2012) Proprotein convertase subtilisin/kexin type 9 interacts with apolipoprotein B and prevents its intracellular degradation, irrespective of the low-density lipoprotein receptor. *Arterioscler. Thromb. Vasc. Biol.* **32,** 1585–1595 CrossRef Medline
21. Romagnuolo, R., Scipione, C. A., Boffa, M. B., Marcovina, S. M., Seidah, N. G., and Koschinsky, M. L. (2015) Lipoprotein (a) catabolism is regulated by proprotein convertase subtilisin/kexin type 9 through the low density lipoprotein receptor. *J. Biol. Chem.* **290,** 11649–11662 CrossRef Medline
22. Fisher, T. S., Lo Surdo, P., Pandit, S., Mattu, M., Santoro, J. C., Wisniewski, D., Cummings, R. T., Calzetta, A., Cubbon, R. M., Fischer, P. A., Tarachandani, A., De Francesco, R., Wright, S. D., Sparrow, C. P., Carfi, A., and Sitlani, A. (2007) Effects of pH and low density lipoprotein (LDL) on PCSK9-dependent LDL receptor regulation. *J. Biol. Chem.* **282,** 20502–20512 CrossRef Medline
23. Galvan, A. M., and Chorba, J. S. (2019) Cell-associated heparin-like molecules modulate the ability of LDL to regulate PCSK9 uptake. *J. Lipid Res.* **60,** 71–84 CrossRef Medline
24. Tavori, H., Rashid, S., and Fazio, S. (2015) On the function and homeostasis of PCSK9: reciprocal interaction with LDLR and additional lipid effects. *Atherosclerosis* **238,** 264–270 CrossRef Medline
25. Fazio, S., Minnier, J., Shapiro, M. D., Tsimikas, S., Tarugi, P., Averna, M. R., Arca, M., and Tavori, H. (2017) Threshold effects of circulating angiopoi-

etin-like 3 levels on plasma lipoproteins. *J. Clin. Endocrinol. Metab.* **102,** 3340–3348 CrossRef Medline
26. Hampton, E. N., Knuth, M. W., Li, J., Harris, J. L., Lesley, S. A., and Spraggon, G. (2007) The self-inhibited structure of full-length PCSK9 at 1.9 Å reveals structural homology with resistin within the C-terminal domain. *Proc. Natl. Acad. Sci. U.S.A.* **104,** 14604–14609 CrossRef Medline
27. Kwon, H. J., Lagace, T. A., McNutt, M. C., Horton, J. D., and Deisenhofer, J. (2008) Molecular basis for LDL receptor recognition by PCSK9. *Proc. Natl. Acad. Sci. U.S.A.* **105,** 1820–1825 CrossRef Medline
28. Seidah, N. G. (2019) The elusive inhibitory function of the acidic N-terminal segment of the prodomain of PCSK9: the plot thickens. *J. Mol. Biol.* **431,** 904–907 CrossRef Medline
29. Ultsch, M., Li, W., Eigenbrot, C., Di Lello, P., Lipari, M. T., Gerhardy, S., AhYoung, A. P., Quinn, J., Franke, Y., Chen, Y., Kong Beltran, M., Peterson, A., and Kirchhofer, D. (2019) Identification of a helical segment within the intrinsically disordered region of the PCSK9 prodomain. *J. Mol. Biol.* **431,** 885–903 CrossRef Medline
30. Holla, Ø. L., Laerdahl, J. K., Strøm, T. B., Tveten, K., Cameron, J., Berge, K. E., and Leren, T. P. (2011) Removal of acidic residues of the prodomain of PCSK9 increases its activity towards the LDL receptor. *Biochem. Biophys. Res. Commun.* **406,** 234–238 CrossRef Medline
31. Jones, D. T. (1999) Protein secondary structure prediction based on position-specific scoring matrices. *J. Mol. Biol.* **292,** 195–202 CrossRef Medline
32. Eisenberg, D., Weiss, R. M., and Terwilliger, T. C. (1982) The helical hydrophobic moment: a measure of the amphiphilicity of a helix. *Nature* **299,** 371–374 CrossRef Medline
33. MacRaild, C. A., Howlett, G. J., and Gooley, P. R. (2004) The structure and interactions of human apolipoprotein C-II in dodecyl phosphocholine. *Biochemistry* **43,** 8084–8093 CrossRef Medline
34. Wierød, L., Cameron, J., Strøm, T. B., and Leren, T. P. (2016) Studies of the autoinhibitory segment comprising residues 31–60 of the prodomain of PCSK9: possible implications for the mechanism underlying gain-of-function mutations. *Mol. Genet. Metab. Rep.* **9,** 86–93 CrossRef Medline
35. Kotowski, I. K., Pertsemlidis, A., Luke, A., Cooper, R. S., Vega, G. L., Cohen, J. C., and Hobbs, H. H. (2006) A spectrum of PCSK9 alleles contributes to plasma levels of low-density lipoprotein cholesterol. *Am. J. Hum. Genet.* **78,** 410–422 CrossRef Medline
36. Verbeek, R., Boyer, M., Boekholdt, S. M., Hovingh, G. K., Kastelein, J. J., Wareham, N., Khaw, K. T., and Arsenault, B. J. (2017) Carriers of the PCSK9 R46L variant are characterized by an antiatherogenic lipoprotein profile assessed by nuclear magnetic resonance spectroscopy—brief report. *Arterioscler. Thromb. Vasc. Biol.* **37,** 43–48 CrossRef Medline
37. Segrest, J. P., Jones, M. K., De Loof, H., Brouillette, C. G., Venkatachalapathi, Y. V., and Anantharamaiah, G. M. (1992) The amphipathic helix in the exchangeable apolipoproteins: a review of secondary structure and function. *J. Lipid Res.* **33,** 141–166 Medline
38. Benjannet, S., Rhainds, D., Hamelin, J., Nassoury, N., and Seidah, N. G. (2006) The proprotein convertase (PC) PCSK9 is inactivated by furin and/or PC5/6A: functional consequences of natural mutations and post-translational modifications. *J. Biol. Chem.* **281,** 30561–30572 CrossRef Medline
39. Kim, D. E., Chivian, D., and Baker, D. (2004) Protein structure prediction and analysis using the Robetta server. *Nucleic Acids Res.* **32,** W526–W531 CrossRef Medline
40. Rohl, C. A., Strauss, C. E., Misura, K. M., and Baker, D. (2004) Protein structure prediction using Rosetta. *Methods Enzymol.* **383,** 66–93 CrossRef Medline
41. Dewpura, T., Raymond, A., Hamelin, J., Seidah, N. G., Mbikay, M., Chrétien, M., and Mayne, J. (2008) PCSK9 is phosphorylated by a Golgi casein kinase-like kinase *ex vivo* and circulates as a phosphoprotein in humans. *FEBS J.* **275,** 3480–3493 CrossRef Medline
42. Chorba, J. S., Galvan, A. M., and Shokat, K. M. (2018) Stepwise processing analyses of the single-turnover PCSK9 protease reveal its substrate sequence specificity and link clinical genotype to lipid phenotype. *J. Biol. Chem.* **293,** 1875–1886 CrossRef Medline
43. Wright, P. E., and Dyson, H. J. (2009) Linking folding and binding. *Curr. Opin. Struct. Biol.* **19,** 31–38 CrossRef Medline
44. Wright, P. E., and Dyson, H. J. (2015) Intrinsically disordered proteins in cellular signalling and regulation. *Nat. Rev. Mol. Cell Biol.* **16,** 18–29 CrossRef Medline
45. Ahrens, J. B., Nunez-Castilla, J., and Siltberg-Liberles, J. (2017) Evolution of intrinsic disorder in eukaryotic proteins. *Cell. Mol. Life Sci.* **74,** 3163–3174 CrossRef Medline
46. Hopkins, P. N., Defesche, J., Fouchier, S. W., Bruckert, E., Luc, G., Cariou, B., Sjouke, B., Leren, T. P., Harada-Shiba, M., Mabuchi, H., Rabès, J. P., Carrié, A., van Heyningen, C., Carreau, V., Farnier, M., *et al.* (2015) Characterization of autosomal dominant hypercholesterolemia caused by PCSK9 gain of function mutations and its specific treatment with alirocumab, a PCSK9 monoclonal antibody. *Circ. Cardiovasc. Genet.* **8,** 823–831 CrossRef Medline
47. Schiele, F., Park, J., Redemann, N., Luippold, G., and Nar, H. (2014) An antibody against the C-terminal domain of PCSK9 lowers LDL cholesterol levels *in vivo*. *J. Mol. Biol.* **426,** 843–852 CrossRef Medline
48. Pisciotta, L., Priore Oliva, C., Cefalù, A. B., Noto, D., Bellocchio, A., Fresa, R., Cantafora, A., Patel, D., Averna, M., Tarugi, P., Calandra, S., and Bertolini, S. (2006) Additive effect of mutations in LDLR and PCSK9 genes on the phenotype of familial hypercholesterolemia. *Atherosclerosis* **186,** 433–440 CrossRef Medline
49. Kaya, E., Kayıkçıoğlu, M., Tetik Vardarlı, A., Eroglŭ, Z., Payzın, S., and Can, L. (2017) PCSK 9 gain-of-function mutations (R496W and D374Y) and clinical cardiovascular characteristics in a cohort of Turkish patients with familial hypercholesterolemia. *Anatol. J. Cardiol.* **18,** 266–272 CrossRef Medline
50. Allard, D., Amsellem, S., Abifadel, M., Trillard, M., Devillers, M., Luc, G., Krempf, M., Reznik, Y., Girardet, J. P., Fredenrich, A., Junien, C., Varret, M., Boileau, C., Benlian, P., and Rabès, J. P. (2005) Novel mutations of the PCSK9 gene cause variable phenotype of autosomal dominant hypercholesterolemia. *Hum. Mutat.* **26,** 497 CrossRef Medline
51. Fasano, T., Sun, X. M., Patel, D. D., and Soutar, A. K. (2009) Degradation of LDLR protein mediated by "gain of function" PCSK9 mutants in normal and ARH cells. *Atherosclerosis* **203,** 166–171 CrossRef Medline
52. Geschwindner, S., Andersson, G. M., Beisel, H. G., Breuer, S., Hallberg, C., Kihlberg, B. M., Lindqvist, A. M., O'Mahony, G., Plowright, A. T., Raubacher, F., and Knecht, W. (2015) Characterisation of *de novo* mutations in the C-terminal domain of proprotein convertase subtilisin/kexin type 9. *Protein Eng. Des. Sel.* **28,** 117–125 CrossRef Medline
53. Sigler, P. B. (1988) Transcriptional activation: acid blobs and negative noodles. *Nature* **333,** 210–212 CrossRef Medline
54. Sugase, K., Dyson, H. J., and Wright, P. E. (2007) Mechanism of coupled folding and binding of an intrinsically disordered protein. *Nature* **447,** 1021–1025 CrossRef Medline
55. Lee, H., Mok, K. H., Muhandiram, R., Park, K. H., Suk, J. E., Kim, D. H., Chang, J., Sung, Y. C., Choi, K. Y., and Han, K. H. (2000) Local structural elements in the mostly unstructured transcriptional activation domain of human p53. *J. Biol. Chem.* **275,** 29426–29432 CrossRef Medline
56. Borcherds, W., Theillet, F. X., Katzer, A., Finzel, A., Mishall, K. M., Powell, A. T., Wu, H., Manieri, W., Dieterich, C., Selenko, P., Loewer, A., and Daughdrill, G. W. (2014) Disorder and residual helicity alter p53-Mdm2 binding affinity and signaling in cells. *Nat. Chem. Biol.* **10,** 1000–1002 CrossRef Medline
57. Krois, A. S., Ferreon, J. C., Martinez-Yamout, M. A., Dyson, H. J., and Wright, P. E. (2016) Recognition of the disordered p53 transactivation domain by the transcriptional adapter zinc finger domains of CREB-binding protein. *Proc. Natl. Acad. Sci. U.S.A.* **113,** E1853–E1862 CrossRef Medline
58. Benjannet, S., Saavedra, Y. G., Hamelin, J., Asselin, M. C., Essalmani, R., Pasquato, A., Lemaire, P., Duke, G., Miao, B., Duclos, F., Parker, R., Mayer, G., and Seidah, N. G. (2010) Effects of the prosegment and pH on the activity of PCSK9: evidence for additional processing events. *J. Biol. Chem.* **285,** 40965–40978 CrossRef Medline
59. Gustafsen, C., Olsen, D., Vilstrup, J., Lund, S., Reinhardt, A., Wellner, N., Larsen, T., Andersen, C. B. F., Weyer, K., Li, J. P., Seeberger, P. H., Thirup, S., Madsen, P., and Glerup, S. (2017) Heparan sulfate proteoglycans present PCSK9 to the LDL receptor. *Nat. Commun.* **8,** 503 CrossRef Medline

60. Benn, M., Nordestgaard, B. G., Grande, P., Schnohr, P., and Tybjaerg-Hansen, A. (2010) PCSK9 R46L, low-density lipoprotein cholesterol levels, and risk of ischemic heart disease: 3 independent studies and meta-analyses. *J. Am. Coll. Cardiol.* **55,** 2833–2842 CrossRef Medline
61. Zhao, Z., Tuakli-Wosornu, Y., Lagace, T. A., Kinch, L., Grishin, N. V., Horton, J. D., Cohen, J. C., and Hobbs, H. H. (2006) Molecular characterization of loss-of-function mutations in PCSK9 and identification of a compound heterozygote. *Am. J. Hum. Genet.* **79,** 514–523 CrossRef Medline
62. Cameron, J., Holla, Ø. L., Ranheim, T., Kulseth, M. A., Berge, K. E., and Leren, T. P. (2006) Effect of mutations in the PCSK9 gene on the cell surface LDL receptors. *Hum. Mol. Genet.* **15,** 1551–1558 CrossRef Medline
63. Millard, C. J., Ludeman, J. P., Canals, M., Bridgford, J. L., Hinds, M. G., Clayton, D. J., Christopoulos, A., Payne, R. J., and Stone, M. J. (2014) Structural basis of receptor sulfotyrosine recognition by a CC chemokine: the N-terminal region of CCR3 bound to CCL11/eotaxin-1. *Structure* **22,** 1571–1581 CrossRef Medline
64. Somers, W. S., Tang, J., Shaw, G. D., and Camphausen, R. T. (2000) Insights into the molecular basis of leukocyte tethering and rolling revealed by structures of P- and E-selectin bound to SLe(X) and PSGL-1. *Cell* **103,** 467–479 CrossRef Medline
65. Tompa, P., Davey, N. E., Gibson, T. J., and Babu, M. M. (2014) A million peptide motifs for the molecular biologist. *Mol. Cell* **55,** 161–169 CrossRef Medline
66. Brown, M. S., and Goldstein, J. L. (2009) Cholesterol feedback: from Schoenheimer's bottle to Scap's MELADL. *J. Lipid Res.* **50,** S15–S27 CrossRef Medline
67. Brown, M. S., Faust, J. R., Goldstein, J. L., Kaneko, I., and Endo, A. (1978) Induction of 3-hydroxy-3-methylglutaryl coenzyme A reductase activity in human fibroblasts incubated with compactin (ML-236B), a competitive inhibitor of the reductase. *J. Biol. Chem.* **253,** 1121–1128 Medline
68. Goldstein, J. L., Basu, S. K., and Brown, M. S. (1983) Receptor-mediated endocytosis of low-density lipoprotein in cultured cells. *Methods Enzymol.* **98,** 241–260 CrossRef Medline
69. Russell, D. W., Brown, M. S., and Goldstein, J. L. (1989) Different combinations of cysteine-rich repeats mediate binding of low density lipoprotein receptor to two different proteins. *J. Biol. Chem.* **264,** 21682–21688 Medline
70. Park, S. W., Moon, Y.-A., and Horton, J. D. (2004) Post-transcriptional regulation of low density lipoprotein receptor protein by proprotein convertase subtilisin/kexin type 9a in mouse liver. *J. Biol. Chem.* **279,** 50630–50638 CrossRef Medline
71. Havel, R. J., Eder, H. A., and Bragdon, J. H. (1955) The distribution and chemical composition of ultracentrifugally separated lipoproteins in human serum. *J. Clin. Invest.* **34,** 1345–1353 CrossRef Medline
72. Rumsey, S. C., Galeano, N. F., Arad, Y., and Deckelbaum, R. J. (1992) Cryopreservation with sucrose maintains normal physical and biological properties of human plasma low density lipoproteins. *J. Lipid Res.* **33,** 1551–1561 Medline
73. Graham, J. M., Higgins, J. A., Gillott, T., Taylor, T., Wilkinson, J., Ford, T., and Billington, D. (1996) A novel method for the rapid separation of plasma lipoproteins using self-generating gradients of iodixanol. *Atherosclerosis* **124,** 125–135 CrossRef Medline
74. Nguyen, M. A., Kosenko, T., and Lagace, T. A. (2014) Internalized PCSK9 dissociates from recycling LDL receptors in PCSK9-resistant SV-589 fibroblasts. *J. Lipid Res.* **55,** 266–275 CrossRef Medline
75. Buchan, D. W., Minneci, F., Nugent, T. C., Bryson, K., and Jones, D. T. (2013) Scalable web services for the PSIPRED Protein Analysis Workbench. *Nucleic Acids Res.* **41,** W349–W357 CrossRef Medline
76. Konrat, R. (2009) The protein meta-structure: a novel concept for chemical and molecular biology. *Cell. Mol. Life Sci.* **66,** 3625–3639 CrossRef Medline